Oxford Medical Case Reports, 2021;8,300–303

https://doi.org/10.1093/omcr/omab065
Case Report

CASE REPORT

Fibroblastic meningioma mimicking an intracerebral hemorrhage: case report

Diego Armando Devia[1,*], David Andrés Armando Devia[2], Eugenio Meek[3], Diego Rivera[4] and Oscar Feo-Lee[1]

[1]Neurosurgery Department, Hospital Universitario San Ignacio, Bogotá, Colombia, [2]Faculty of Medicine, Hospital Universitario San Ignacio, Bogotá, Colombia, [3]Pathology Department, Hospital Universitario San Ignacio, Bogotá, Colombia, [4]Radiology Department, Hospital Universitario San Ignacio, Bogotá, Colombia

*Correspondence address. Neurosurgery Department, Hospital Universitario San Ignacio, Bogotá 110111, Colombia. Tel: +57 3138097829; Fax: 5946161, Ext. 2419; E-mail: diego.devia54@gmail.com

Abstract

A 50-year-old woman presented to the emergency room complaining of severe headache. A non-contrasted head CT was obtained, which demonstrated a hyperdense image compatible with an intracerebral hemorrhage in the posterior region of the left temporal lobe. The patient displayed no neurological deficit during the consultation and a subsequent MRI showed a temporoinsular bleeding lesion that was suggestive of an atypic meningioma or a metastatic lesion. Afterwards, neck, chest and abdomen CT scans were performed, and the imaging ruled out a secondary neoplasm. The patient underwent surgical resection of the lesion, and a solid tumor was found with no bleeding associated. The pathology reported a WHO I fibroblastic meningioma.

INTRODUCTION

Hemorrhagic strokes account for 15% of all strokes and are widely accepted to be deadlier than ischemic strokes. The 30-day mortality rate of patients presenting intracranial hemorrhage is ∼50%, in comparison with an estimated 20% rate for patients that have experienced ischemic strokes [1].

The most common cause of intra-parenchymal hemorrhage is thought to be chronic hypertension. The small perforating end branches are especially vulnerable to damage from elevated blood pressure in locations such as the basal ganglia, thalamus, cerebellum, brainstem and pons.

Although all brain tumors are known to convey a risk of bleeding, medical teams tend to associate tumoral intra-cerebral hemorrhages with the presence of malignancies. The types of malignant tumors that are most associated with localized hemorrhages are glioblastomas, lymphomas, oligodendrogliomas and metastatic tumors, the last of which encompass melanomas, choriocarcinomas, renal cell carcinomas and bronchogenic carcinomas [2, 3]. Contrastingly, the types of benign tumors that have been associated with intracerebral hemorrhages include meningiomas, pituitary adenomas and hemangioblastomas [4, 5].

The factors that determine the prognosis and severity of a hemorrhagic stroke include the size of the hemorrhage, the patient's age, the Glasgow Coma Scale score, the location of hematoma and the presence of an intra-ventricular component. All the aforementioned factors are also considered to calculate the intracranial hemorrhage score [6].

CASE REPORT

A 50-year-old patient presented to the emergency room complaining of having suffered, for an entire day, from a sudden pulsatile hemicranial headache of moderate intensity, associated with nausea, no emetic episodes and that was also not responding to the use of acetaminophen or NSAIDs. Due to the

Received: December 20, 2020. **Revised:** June 30, 2021. **Accepted:** July 6, 2021

Figure 1: Head computerized tomography CT.

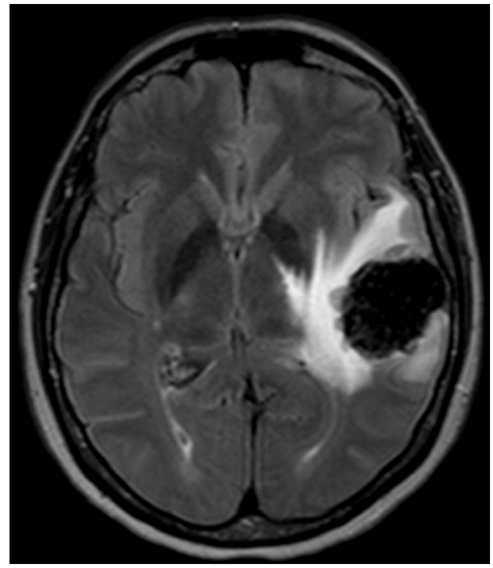

Figure 2: MRI—fluid attenuated inversion recovery (FLAIR) sequence.

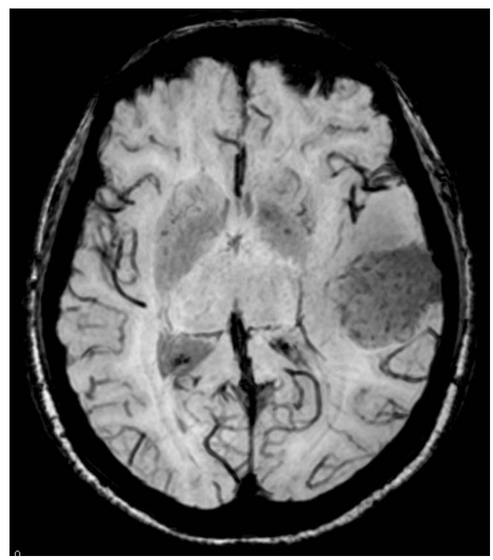

Figure 3: MRI—susceptibility weighted imaging (SWI) sequence.

persistence of the symptomatology, the patient sought medical attention and the initial diagnosis suggested a secondary headache. After careful examination, the patient was found to be free of neurological deficit and the medical team performed a brain CT scan.

The resulting image documented a cortico-subcortical hyperdense lesion (50 Hounsfield Units) in the posterior region of the left temporal lobe, measuring $41 \times 32 \times 36$ mm and with an approximate volume of 24.5 cc, commonly associated with cases of vasogenic edema compromising the posterior limb of the internal capsule. The amplitude of the left lateral ventricle and the width of the regional subarachnoid space sulci had decreased on account of the lesion, and a minimal deviation of the midline structures to the right and incipient left uncal herniation was noted. (Fig. 1). To rule out an underlying vascular malformation, the medical team performed a CT angiogram, which did not show any aneurysms or arteriovenous malformations.

Due to the absence of neurological deficit, the medical team propounded that a brain hemorrhage could not be adjudged as the sole etiology and subsequently ordered an MRI scan. The results revealed a lobulated mass with prominent enhancement after the gadolinium injection and marked hypo intensity in the magnetic resonance sequences with T2 information. A zone in contact with the internal bone table was observed at the lateral margin of the lesion, as well as various dark regions at the susceptibility weighted sequence, suggesting blood products or calcium. The FLAIR sequence showed significant surrounding vasogenic edema. The aforementioned characteristics were found to be consistent with an atypical meningioma or a metastatic lesion (Figs 2–4).

Additional neck, chest and abdominal CT scans were performed, and the results allowed the ruling out of metastatic disease, furthermore, increasing the probability of an underlying primary tumor of the central nervous system. The patient underwent surgery, where resulted in the identification of a solid lesion, without an intra-tumoral hemorrhagic component, as previously suspected in accordance with the pre-operative imaging findings (Figs 5 and 6).

After the surgical intervention, the patient presented a stable neurological evolution with no apparent deterioration and was discharged following 4 days of post-operative surveillance. During the post-operative follow-up, the pathology report revealed the existence of spindle cells fascicles intersected along with variable collagen deposition and occasional cellular whorls (in the hematoxylin–eosin staining—Fig. 7). The tumor also tested positive for EMA in patches and Vimentin (Fig. 8). These findings were deemed compatible with the diagnosis of fibroblastic meningioma WHO I, emphasizing that they were not suggestive of anaplastic meningioma or atypical meningioma.

DISCUSSION

The radiological findings in this case are particularly intriguing, due to the fact that the initial evaluation suggested a large acute hemorrhagic component—because of its high density in scans (50 Hounsfield Units) and its marked hypointensity in the magnetic resonance sequences with T2 information—but, at the time of the surgical resection, a mass of solid consistency was found, without any type of hemorrhage.

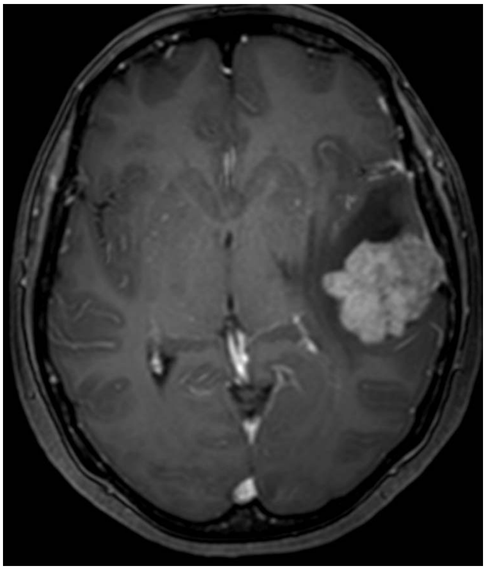

Figure 4: MRI—gadolinium-enhanced T1-weighted sequence.

Figure 5: Macroscopic lesion.

Figure 6: Macroscopic lesion.

Given that acute blood is markedly hyperdense in comparison to the brain parenchyma, its tomographic diagnosis regularly does not pose a high grade of difficulty for medical teams. However, in this case, we were faced with an entirely solid lesion that mimicked an intracerebral hemorrhage. The tests ordered by the medical team included a CT angiogram to rule out a possible vascular etiology, as the patient's symptomatology

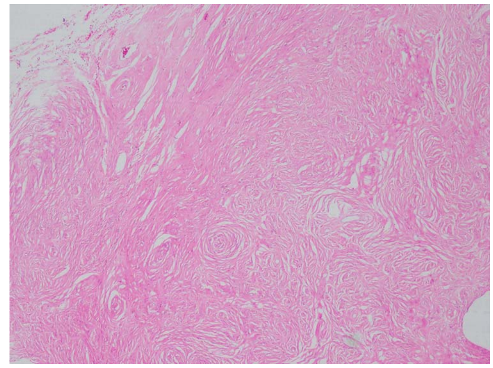

Figure 7: Hematoxylin–eosin staining.

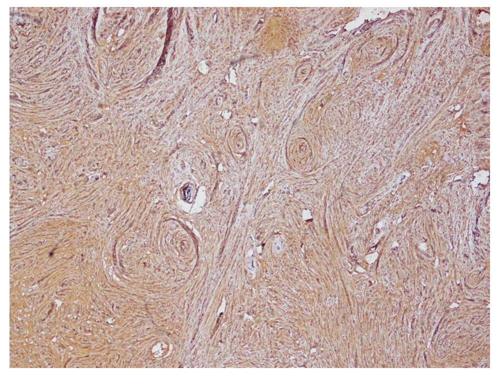

Figure 8: Vimentin staining.

was not consistent with a primary hemorrhage. In the authors' opinion, this is the most significant aspect of this case study, in terms of its possible contribution to medical literature and its potential of serving as reference material for other healthcare professionals assessing patients who report a similar array of symptoms.

In developing nations, medical institutions are typically constrained by multiple external factors that directly compromise the availability of primary imaging techniques, such as MRI scanning. In cases where diagnostic MRI equipment is found to be entirely unavailable, medical teams must judiciously evaluate each patient's condition, to determine whether he should be immediately referred to a higher level facility or remain under surveillance after a CT scan. In this case, the patient presented to the ER with a diagnosis of a 'large intracerebral hemorrhage' but displayed no neurological deficit. Such a scenario was deemed unlikely by the medical team, given the absence of cognitive impairment, and thus, the symptoms were thought to be the result of a slow-growing lesion.

In accordance with the findings of this case, the authors pose that all medical teams evaluating the results of a Head CT scan must consider the correlation between the images and the patient's neurological status (i.e. a patient with no neurological deficit, associated with a large hyperdense lesion, most probably relates to a tumor with intra-lesional hemorrhage, rather than a single hemorrhage). Additionally, this case allowed the authors to identify a valuable opportunity in the development of a computer-based algorithm—specially directed at medical centers with CT scanners, but lacking MRI imaging equipment—which marks the cases in which an extra imaging study should be ordered, starting with those 'hyperdense lesions' located in eloquent areas with no neurological deficit association.

As it was stated before, the patient's neurological status during admission was undamaged, which is highly unlikely in patients with hemorrhages in the same location and with an approximate volume of 24.5 cc. Had that been the case for our patient, at least, a minimum degree of neurological compromise would have been expected, as the volume of intra-parenchymal hemorrhage is directly proportional to morbidity and mortality [7].

Type III collagen is a member of the fibrillar collagen family and is colocalized with the most abundant member of the family, type I collagen, in such tissues as blood vessels [8], leading the medical team to the conclusion that the high content of intercellular collagen and reticulin was the most probable cause for the hyperdensity evidenced in the tomographic image and the hypodensity on T2 weighted images, and for the dark areas evidenced on the susceptibility weighted images, thereby mimicking an intra-parenchymal hemorrhage.

ACKNOWLEDGMENTS

The authors gratefully acknowledge the assistance of Julian Gualdrón-Durán in the edition and preparation of this manuscript.

CONFLICT OF INTEREST STATEMENT

None declared.

FUNDING

None declared.

ETHICAL APPROVAL

The case report was reviewed and accepted by the institutional review board from our institution.

CONSENT

Full verbal and written informed consent has been obtained from the patient for submission of this manuscript for publication.

GUARANTOR

Dr Oscar Hernando Feo-Lee is acting as a guarantor for this manuscript.

REFERENCES

1. Sacco S, Marini C, Toni D, Olivieri L, Carolei A. Incidence and 10-year survival of intracerebral hemorrhage in a population-based registry. *Stroke* 2009;**40**:394–9. https://doi.org/10.1161/STROKEAHA.108.523209 Epub 2008 Nov 26 PMID: 19038914.
2. Scott M. Spontaneous intracerebral hematoma caused by cerebral neoplasms. *J Neurosurg* 1975;**42**:338–42.
3. Dublin AB, Norman D. Fluid-fluid level in cystic cerebral metastatic melanoma. *J Comput Assist Tomogr* 1979;**3**: 650–2. https://doi.org/10.1097/00004728-197910000-00014 PMID: 479417.
4. Modesti LM, Binet EF, Collins GH. Meningiomas causing spontaneous intracranial hematomas. *J Neurosurg* 1976;**45**:437–41. https://doi.org/10.3171/jns.1976.45.4.0437 PMID: 956880.
5. Little JR, Dial B, Belanger G, *et al*. Brain hemorrhage from intracranial tumor. *Stroke* 1979;**10**:283–8.
6. Hemphill JC, Bonovich DC, Besmertis L, *et al*. The ICH score: a simple, reliable grading scale for intracerebral hemorrhage. *Stroke* 2001;**32**:891–7 A.
7. Broderick JP, Brott TG, Duldner JE, Tomsick T, Huster G. Volume of intracerebral hemorrhage - a powerful and easy to use predictor of 30-day mortality. *Stroke* 1993;**24**: 987–93.